Computational fluid dynamic evaluation of the side-to-side anastomosis for arteriovenous fistula

Jeffrey E. Hull, MD,[a] Boris V. Balakin, PhD,[b] Brad M. Kellerman, BSc,[c] and **David K. Wrolstad, BSc,[c]**
North Chesterfield, Va; Bergen, Norway; and San Juan Capistrano, Calif

Objective: **The goal of this research was to compare side-to-side (STS) and end-to-side (ETS) anastomoses in a computer model of the arteriovenous fistula with computational fluid dynamic analysis.**
Methods: **A matrix of 17 computer arteriovenous fistula models (SolidWorks, Dassault Systèmes, France) of artery-vein pairs (3-mm-diameter artery + 3-mm-diameter vein and 4-mm-diameter artery +6-mm-diameter vein elliptical anastomoses) in STS, 45° ETS, and 90° ETS configurations with cross-sectional areas (CSAs) of 3.5 to 18.8 mm^2 were evaluated with computational fluid dynamic software (STAR-CCM+; CD-adapco, Melville, NY) in simulations at defined flow rates from 600 to 1200 mL/min and mean arterial pressures of 50 to 140 mm Hg. Models and configurations were evaluated for pressure drop across the anastomosis, arterial inflow, venous outflow, arterial outflow, velocity vector, and wall shear stress (WSS) profile.**
Results: **Pressure drop across the anastomosis was inversely proportional to anastomotic CSA and to venous outflow and was proportional to arterial inflow. Pressure drop was greater in 3 + 3 models than in 4 + 6 STS models; 90° ETS configurations had the lowest pressure drops and were nearly identical, whereas 45° ETS configurations had the highest pressure drops. Venous outflow in the 4 + 6 model in STS configurations, evaluated at 100 mm Hg arterial inflow pressure, was 390, 592, 610, and 886 mL/min in anastomotic CSAs of 3.5, 5.3, 7.1, and 18.8 mm^2, respectively, and was similar in 90° ETS (609 and 908 mL/min) and lower in 45° ETS (534 and 562 mL/min) configurations at CSAs of 5.3 and 18.8 mm^2. The mean increase in venous outflow was 69 mL/min (range, −59 to 134) between 3 + 3 and 4 + 6 models at 100 mm Hg arterial inflow. The most uniform WSS profile occurs in STS anastomoses followed by 45° ETS and then 90° ETS anastomoses.**
Conclusions: **The STS and 90° ETS anastomoses have high venous outflow and a tendency toward reversed arterial outflow. The 45° ETS anastomosis has reduced venous outflow but resists reversed arterial outflow. The STS anastomosis has more uniform WSS characteristics compared with the 45° and 90° ETS anastomoses. (J Vasc Surg 2013;58:187-93.)**

Clinical Relevance: **The vascular anastomosis is a fundamental technique in vascular surgery and has many variations. Computational fluid dynamic simulations can define the optimal type, size, and shape of the anastomosis and predict intimal hyperplasia using wall shear stress analysis. Computational fluid dynamic modeling and analysis can guide surgeons to obtain better technical and clinical results when performing the vascular anatomosis. This article examines computational fluid dynamic simulations of the side-to-side anastomoses and two configurations of end-to-side anastomoses.**

There is increasing evidence that anatomy and type of anastomosis can affect the flow and the development of intimal hyperplasia in arteriovenous fistulas (AVFs).[1,2] One effective tool in the evaluation of these effects is computational fluid dynamics (CFD). CFD has been used to predict flow, pressure, velocity, and wall shear stress (WSS) in AVFs. This study compares the CFD characteristics of side-to-side (STS) and end-to-side (ETS) anastomoses between vessels that are straight, parallel, and in close proximity, in terms of flow, pressure, velocity vector, and WSS, in an attempt to predict optimum anastomosis geometry, size, potential for maturation, and development of intimal hyperplasia. A recent study reported improved results with a STS anastomosis. In the piggyback straight line onlay technique (pSLOT), straight and parallel vessels are brought together without bending or twisting and are joined with a STS anastomosis. The pSLOT technique has been reported to yield a significant reduction in surgical arteriovenous fistula (sAVF) failure ascribed to the STS anastomosis and straight and parallel anatomy of the vessels.[3] The results for pSLOT are preliminary, and one reason for undertaking CFD analysis of the STS anastomosis is to see if flow and WSS contribute to improved results. A STS anastomosis with similar vessel anatomy has been proposed in the creation of a percutaneous arteriovenous fistula using in situ vessels that are in direct contact or in close proximity to one another (Hull JE. The percutaneous arteriorvenous fistula (pAVF). Presented at the Vascular Access Society of America meeting. Orlando, Fla, May 2012.)

From the Richmond Vascular Center, North Chesterfield[a]; the University of Bergen, Bergen[b]; and Caymus Medical, San Juan Capistrano.[c]
Author conflict of interest: none.
Additional material for this article may be found online at www.jvascsurg.org.
Reprint requests: Jeffrey E. Hull, MD, Richmond Vascular Center, 173 Wadsworth Dr, North Chesterfield, VA 23236 (e-mail: jhull@richmondvascularcenter.com).
The editors and reviewers of this article have no relevant financial relationships to disclose per the JVS policy that requires reviewers to decline review of any manuscript for which they may have a conflict of interest.
0741-5214/$36.00

http://dx.doi.org/10.1016/j.jvs.2012.10.070

METHODS

A matrix of 17 model AVFs (Table) was created in SolidWorks (Dassault Systèmes, France). Models consisted of artery-vein pairs: 3-mm-diameter artery + 3-mm-diameter vein (3 + 3) or 4-mm-diameter artery + 6-mm-diameter vein (4 + 6). The vessels were straight, parallel, and in close proximity. The anastomotic angle in ETS anastomoses was 45° or 90°. Anastomoses were elliptical with dimensions (length × width) of 3.0 × 1.5, 4.5 × 1.5, 6.0 × 1.5, and 6.0 × 4.0 corresponding to cross-sectional areas (CSAs) of 3.5, 5.3, 7.1, and 18.8 mm^2. Anastomosis size was chosen to represent a range of sizes likely to simulate the end result from anastomosis of a 3 + 3 artery-vein pair in the creation of an AVF. The 6.0 × 4.0-mm anastomosis was specifically chosen to allow comparison with Van Canneyt and colleagues' study[2] of anastomosis angle in ETS anastomoses. The smallest anastomoses, 3.0 × 1.5 mm, were studied to test the lower practical limit of anastomosis size. Anastomotic configurations were STS with distal vein occlusion 5 mm distal to anastomosis (STS), STS with short distal vein occlusion (short STS), STS with open distal vein (open STS), ETS with 45° anastomotic angle (45° ETS), and ETS with 90° anastomotic angle (90° ETS).

The AVFs were analyzed for pressure drop across the anastomosis at flow rates of 600, 750, 900, 1050, and 1200 mL/min. Pressure drop is an inverse measure of potential flow through an anastomosis and reflects whether adequate flow for dialysis can be achieved. Flow rates were chosen to represent flows suitable for dialysis and potentially achievable with the vessel size modeled. The pressures were obtained 2.5 mm from the anastomosis in the arterial inflow (A_i) and the proximal venous outflow (V_o). A distance of 2.5 mm allows calculation of pressure away from virtual turbulence caused by anastomosis in the CFD model. Flow was distributed 92% to the V_o and 8% to the arterial outflow (A_o) as described by Van Canneyt et al.[2] Velocity vector and WSS maps were created for each model at each flow rate.

The 45° ETS, short STS, and open STS configurations of both 3 + 3 and 4 + 6 vessel models were analyzed for A_i, A_o, and V_o flow at constant mean arterial pressures of 50, 60, 80, 100, 120, and 140 mm Hg. In the open model, distal venous outflow flow (V_d) was also recorded.

Computational fluid dynamic analysis and boundary conditions. Computer-aided design models produced in SolidWorks (Dassault Systèmes, France) were further imported into STAR-CCM+ (Version 5.06.010; cd-Adapco, Melville, NY) via Initial Graphic Exchange Specified surfaces. There were 30,000 to 45,000 regular computational grids (depending on the flow configuration) of 1-mm average base size built on the surfaces with the use of a built-in trimmed mesher. The AVF region was refined with the trimmed cells to an average size of 0.2 mm.

Computational fluid dynamic parameters were mathematically defined as previously described (see equations in the Appendix, online only).[2,4,5]

Two sets of the side boundary conditions were applied to the model. The first set with the constant-velocity inlet and the designated flow split arterial 8% and venous 92% outlets was used for the determination of pressure drops, WSS, and velocity profiles in the AVF region. The constant-velocity inlet assumes the flow to be nonpulsatile. However, the inlet flow rates were changed in the interval 600-1200 mL/min to mimic pulsations as a best approximation.

The flow rates in the model were mapped with the use of pressure boundaries at the sides. The pressure at the arterial inlet was 100 mm Hg; the venous outlet pressure was then defined taking into account the AVF pressure drop computed at the first stage of modeling. The arterial outlet pressure was selected so that the entire flow rate through the model was close to 900 mL/min. It must be noted that the artificial selection of arterial outlet pressure brings an additional degree of freedom to the model.

The rest of the model periphery was set up to be a rigid no-slip wall.

Computational fluid dynamic equations were discretized in STAR-CCM+ and iterated with the steady SIMPLE solver until the maximum residual was not less than 10^{-6}.

Table. Model, anastomosis size, and configuration matrix[a]

Model (artery + vein)	*Size, mm*	*STS*	*Short STS*	*Open STS*	*45° ETS*	*90° ETS*
3 + 3	3.0 × 1.5	X				
3 + 3	4.5 × 1.5	X	X	X	X	X
3 + 3	6.0 × 1.5	X				
4 + 6	3.0 × 1.5	X				
4 + 6	4.5 × 1.5	X	X	X	X	X
4 + 6	6.0 × 1.5	X				
4 + 6	6.0 × 4.0	X			X	X

STS, Side-to-side; *ETS*, end-to-side.

[a]Matrix covers 17 evaluations of models of two artery-vein pairs, either 3-mm artery and 3-mm vein (3 + 3) or 4-mm artery and 6-mm vein (4 + 6). The standard STS anastomosis was tested in all models and anastomosis sizes. Different anastomotic configurations (short STS, open STS, 45° ETS, and 90° ETS) were tested with both artery-vein pair models using a 4.5 × 1.5-mm anastomosis. The 45° ETS and 90° ETS anastomotic configurations were also tested in the 4+6 model using a 6.0 × 4.0-mm anastomosis.

RESULTS

Pressure drop across the anastomosis is inversely proportional to anastomosis CSA and to venous outflow and is proportional to arterial inflow. STS and 90° ETS configurations had the lowest pressure drops and were nearly identical, whereas the 45° ETS configuration had the highest (Fig 1). In the STS anastomosis, mean venous outflow increased with anastomosis CSA from 390 mL/min at 3.5 mm^2 CSA to 886 mL/min at 18.8 mm^2 CSA in the 3 + 3 model and increased by an average of 93 mL/min (standard deviation [SD], 32) in the larger 4 + 6 model ($P = .86$). Venous outflow in anastomoses of 5.3-mm^2 CSA in the 3 + 3 model was 435-729 mL/min (45° ETS, 90° ETS, and STS), and that in the 4 + 6 model was 534-863 mL/min (45° ETS, 90° ETS, and STS). Reversed arterial outflow occurred with STS and 90° ETS configurations with CSA 18.8 mm^2, but not other sizes or

configurations. CFD analysis of our anastomosis matrix showed that the most uniform WSS profile occurs in STS anastomoses followed by 45° and then 90° ETS anastomoses.

Pressure drop. The pressure drop across the anastomosis increases with fistula flow (600-1200 mL/min) for all models and configurations. Pressure drop across the anastomosis is inversely proportional to anastomosis CSA. Pressure drop is also inversely proportional to venous outflow in all configurations except the open STS. Mean pressure drop was 62 mm Hg (range, 17-142; SD, 30) in the 3 + 3 models and 32 mm Hg (range, 10-71; SD, 16) in the 4 + 6 models with the same anastomotic CSA and configuration (ie, excluding 6.0 × 4.0-mm anastomosis in 4 + 6 model). The lowest pressure drops were in the 4 + 6 model of the 6.0 × 4.0-mm anastomosis in the STS and 90° ETS configurations, followed by the 45° ETS configuration (Fig 1).

Anastomotic configuration can significantly affect pressure drop. Pressure drop is most prominently affected by anastomotic angle. The 45° ETS configuration of a 5.3-mm^2 (4.5 × 1.5 mm) anastomosis has an average 42 mm Hg drop compared with 34 mm Hg for the STS configuration of a 3.5-mm^2 anastomosis. In the remaining smaller anastomoses, the pressure drops from low to high were: STS 6.0 × 1.5, STS 4.5 × 1.5, open STS 4.5 × 1.5, short STS 4.5 × 1.5, STS 3.0 × 1.5, 90° ETS 4.5 × 1.5, and 45° ETS 4.5 × 1.5. A similar pattern was observed for the 45° ETS, 90° ETS, and STS configurations of the large 18.8-mm ^{2} (6.0 × 4.0 mm) anastomosis, yielding drops of 15, 7, and 6 mm Hg, respectively.

Venous outflow. Venous outflow at an arterial pressure of 100 mm Hg increased from the 3 + 3 model to the 4 + 6 model. Mean venous outflow for all configurations of 4.5 × 1.5-mm anastomoses in the 3 + 3 model was 562 mL/min (range, 435-729; SD, 103) and increased in the 4 + 6 model to 611 mL/min (range, 534-863; SD, 143). This increase was not statistically significant ($P = .44$, two-tailed f test). Venous outflow from lowest to highest by configuration was 45° ETS, standard STS, 90° ETS, short STS, open STS in both the 3 + 3 and 4 + 6 models (Fig 2).

In the 3 + 3 model of 4.5 × 1.5-mm anastomoses, venous outflow was 729, 622, 523, 498, and 435 mL/min in the open STS, short STS, STS, 90° ETS, and ETS 45° configurations, respectively. There was little change with increase in CSA from 3.5 to 7.1 mm in the STS configuration. In the 4 + 6 model of 4.5 × 1.5-mm anastomoses, venous outflow was 863, 678, 609, 592, and 534 mL/min in the open STS, short STS, 90° ETS, STS, and 45° ETS configurations, respectively. There was increased venous outflow when compared with the 3 + 3 models in all configurations except the smallest STS configuration of a 3.0 × 1.5-mm anastomosis. Flow shows a linear rise with increasing mean arterial inflow pressures of 50, 60, 80, 100, 120, and 140 mm Hg, in all models and configurations. In the 4 + 6 model of the largest anastomosis, 18.8 mm^2 (6.0 × 4.0 mm), there is reversed arterial outflow in the STS and 90° ETS configurations.

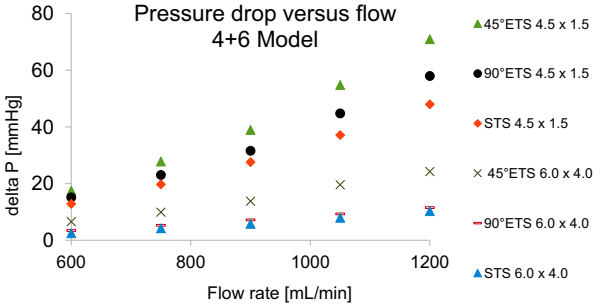

Fig 1. Pressure drop across anastomoses at flow rates of 600 to 1200 mL/min in 4 + 6 artery-vein pair models in three configurations (side-to-side [*STS*] and 45° and 90° end-to-side [*ETS*]) and two sizes of anastomosis (4.5 × 1.5 and 6.0 × 4.0 mm).

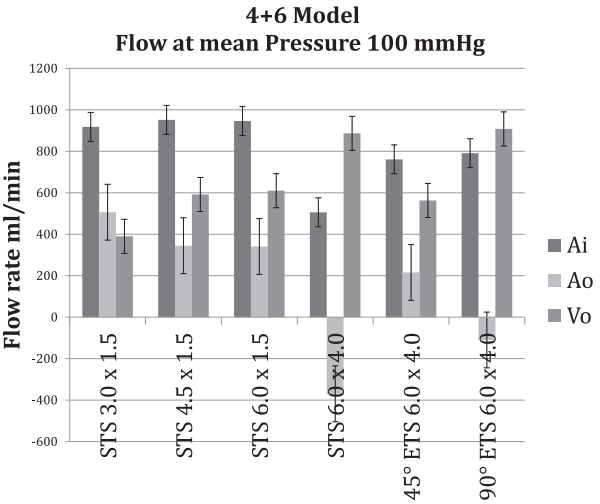

Fig 2. Histograms of flow at an inlet pressure of 100 mm Hg showing arterial inflow (A_i), arterial outflow (A_o), and proximal venous outflow (V_o), in milliliters per minute, with side-to-side (*STS*) and 45° and 90° end-to-side (*ETS*) configurations of 3.0 × 1.5-, 4.5 × 1.5-, and 6.0 × 4.0-mm anastomoses.

WSS. Velocity vector and WSS maps for 3 + 3 models reveal the uniform appearance of the WSS diagrams increasing in magnitude as flow increases. In the 4 + 6 models WSS diagrams remain uniform, but overall WSS is reduced with increased vessel size when compared with 3 + 3 models. Velocity vector and WSS profiles in STS anastomoses show increased flow and continued uniform but less intense WSS profiles as anastomoses increase from 3.5 to 7.1 cm^2 in both 3 + 3 and 4 + 6 models (Fig 3). Paired velocity vector and WSS maps for the 4 + 6 model of an 18.8-mm^2 CSA (6.0 × 4.0 mm) anastomosis at a constant flow rate of 900 mL/min show the most uniform WSS in the STS configuration followed by the 45° ETS, and the most heterogeneous in the 90° ETS configuration (Fig 4).

DISCUSSION

CFD has been used to evaluate pressure, flow, anastomotic CSA, anastomotic angle, velocity vector, WSS

profile, and the development of intimal hyperplasia in AVFs.[1,2,4] Validation of several models has been performed in vitro and in vivo in animal and human models.[1,4-7] We purposely replicated Van Canneyt and colleagues' model and configuration as a way to validate our results and provide an extended comparison of STS and ETS anastomoses.[2] In the 4 + 6 model of 6.0 × 4.0-mm anastomoses in the 45° and 90° ETS anastomoses, our findings in evaluating pressure drop and venous outflow matched the results in the same model and configurations of Van Canneyt et al.[2]

The current CFD study of AVFs has provided some insight into the use of STS anastomoses in the AFV model. It has shown STS anastomoses to be efficient with low-pressure drop from artery to vein and good venous outflow, but also revealed the tendency for steal phenomenon with reversed arterial outflow with large 6.0 × 4.0-mm anastomoses. The STS and 90° ETS both share this characteristic of good pressure drop and venous outflow but reversed arterial outflow that was described by Van Canneyt et al.[2] The 45° ETS anastomosis had the highest pressure drop across the anastomosis, the lowest venous outflow, and an intermediate WSS profile.

The main difference between the STS and ETS anastomoses is found in the WSS profiles. WSS in the STS models was decreased in intensity and more uniform than in the ETS configurations, especially the 90° ETS configuration. The importance of WSS is that this is the variable most closely associated with intimal hyperplasia as described in several CFD studies.[1,4-6] The uniform WSS profile of the STS configuration may be partly responsible for the decreased intimal hyperplasia described with the pSLOT anastomosis that decreased wrist fistula failure rate from 40% to 17%.[3]

The 3 + 3 and 4 + 6 models were selected to represent the physiological changes possible after creation of the AVF where there is increase in flow and vessel size within 15 to 30 minutes.[6,8] In our study, the increase in vessel size after AVF is associated with mild but statistically insignificant venous outflow. Ramacciotti et al, in a canine model of STS fistula, obtained mean venous outflows of 397 mL/min with an anastomosis length 1.5 times the arterial diameter and 629 mL/min with an anastomosis length 3.0 times the arterial diameter.[8] Our model was consistent with this data for animals, yielding venous outflows of 449, 523, and 533 mL/min in anastomoses 1, 1.5, and 2 times the length of the arterial diameter in the 3 + 3 model.

The open STS configuration was interesting in that it gave the highest proximal venous outflow without showing a significantly lower pressure drop. Additionally, it seems the flow in the distal vein would reduce the amount of flow available for the proximal vein. A possible explanation is that model had two degrees of freedom as a venous "inlet" pressure was also specified, adding additional uncertainty to the model.

Clinical application. To make use of the STS anastomosis for AVFs in humans, suitable anatomy is required. In an ultrasound anatomic study of artery-vein pairs in the arm with vessels ≥2 mm in diameter, straight, within 1.5 mm of each other, and relative vessel axis less than 30°, we found that 47.6% (30 of 63) of dialysis patients had suitable anatomy at the snuffbox, and 87.9% (29 of 33) at the elbow (author's unpublished data under review). In addition to patient anatomy, other factors such as the amount of dissection required, the angle between the joined vessels, and the final size and shape of the anastomosis (as opposed to idealized ellipse) are likely to come into play.

Concepts from this study that could be applied to creating an AVF include anastomotic sizing to achieve appropriate venous outflow, anastomotic and vessel wall geometric configurations to limit intimal hyperplasia, anastomotic configuration to prevent reversed arterial outflow and steal phenomenon, effect of proximal side branches, and treatment of the distal vein segment in STS anastomoses.

The STS and 90° ETS anastomoses both give excellent venous outflow. In a canine study, venous outflow rapidly increased 5- and 10-fold over the initial arterial inflow in AVFs with STS anastomoses with lengths 1.5 and 3.0 times the initial artery diameter, respectively.[8] Our STS anastomosis data correlates well with the marginal flow of <400 mL/min achieved with the 3.0 × 1.5-mm anastomosis, the acceptable flow around 600 mL/min achieved with the 4.5 × 1.5-mm anastomosis, and the good flow of 800 mL/min achieved with the 6.0 x 4.0-mm anastomosis. The 90° ETS configuration mirrored the STS venous outflow results. The 45° ETS configuration achieved a venous outflow of only 562 mL/min with a 6.0 × 4.0-mm anastomosis.

Intimal hyperplasia has been correlated with WSS. Areas of high WSS cause positive vessel remodeling (enlargement) and are desirable. Heterogeneous WSS causes intimal hyperplasia to develop in areas of relative low WSS. Uniform and high WSS should give the least intimal hyperplasia.

Reversed arterial outflow is a common phenomenon in the STS anastomosis as shown by Ramacciotti et al.[8] In our model, the STS and 90° ETS anastomoses behaved similarly (Fig 2). ETS anastomosis angles between 3° and 58° do not yield reversed arterial flow in CFD models with arterial inflow of 900 mL/min.[2]

The open configuration simulates not tying off the distal vein of a STS anastomosis. This configuration is also an example of a large proximal side branch. This study examines the AVF in what would be considered the proximal venous segment, so the effect of side branches in other portions of a fistula cannot be commented on. The open configuration was interesting because it has the highest venous outflow, 729 and 863 mL/min, for 4.5- × 1.5-mm anastomoses in the 3 + 3 and 4 + 6 models. In our model the open distal vein or side branch appears to lead to an overall increase in flow.

The short configuration evaluates the effect of obstructing the distal vein closer to the anastomosis. The differences were increases of 98 and 86 mL/min in the 3 + 3 and 4 + 6 models. This suggests that change in the distal vein length or geometry by spatulation could be relevant.

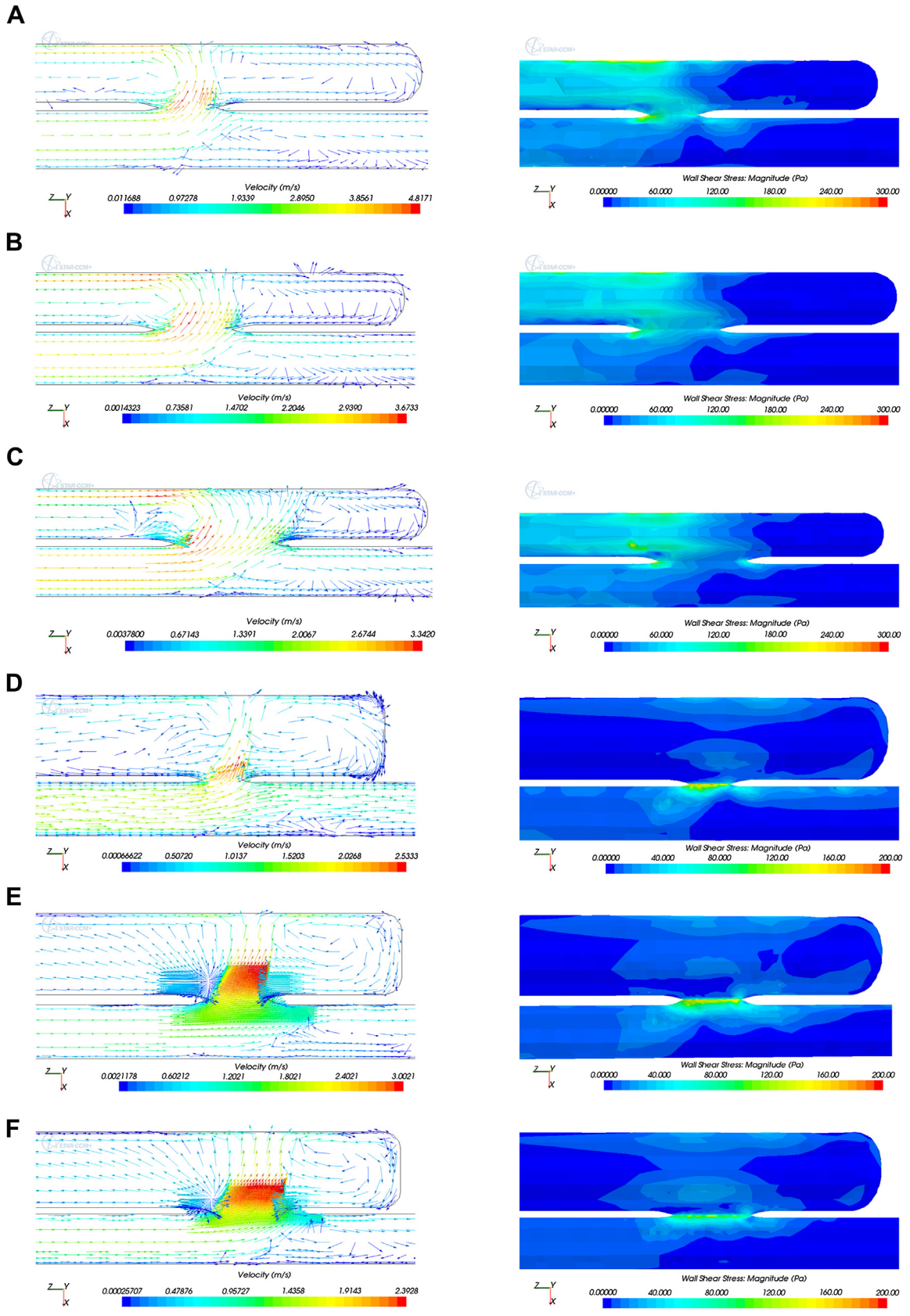

Fig 3. Paired velocity vector and wall shear stress (WSS) diagrams of side-to-side (STS) anastomoses at a constant flow rate of 900 mL/min. **A-C**, 3 + 3 vein-pair models of 3.0- × 1.5-mm, 4.5- × 1.5-mm, and 6.0- × 1.5-mm anastomoses, respectively. **D-F**, 4 + 6 vein-pair models of 3.0- × 1.5-mm, 4.5- × 1.5-mm, and 6.0- × 1.5-mm anastomoses, respectively.

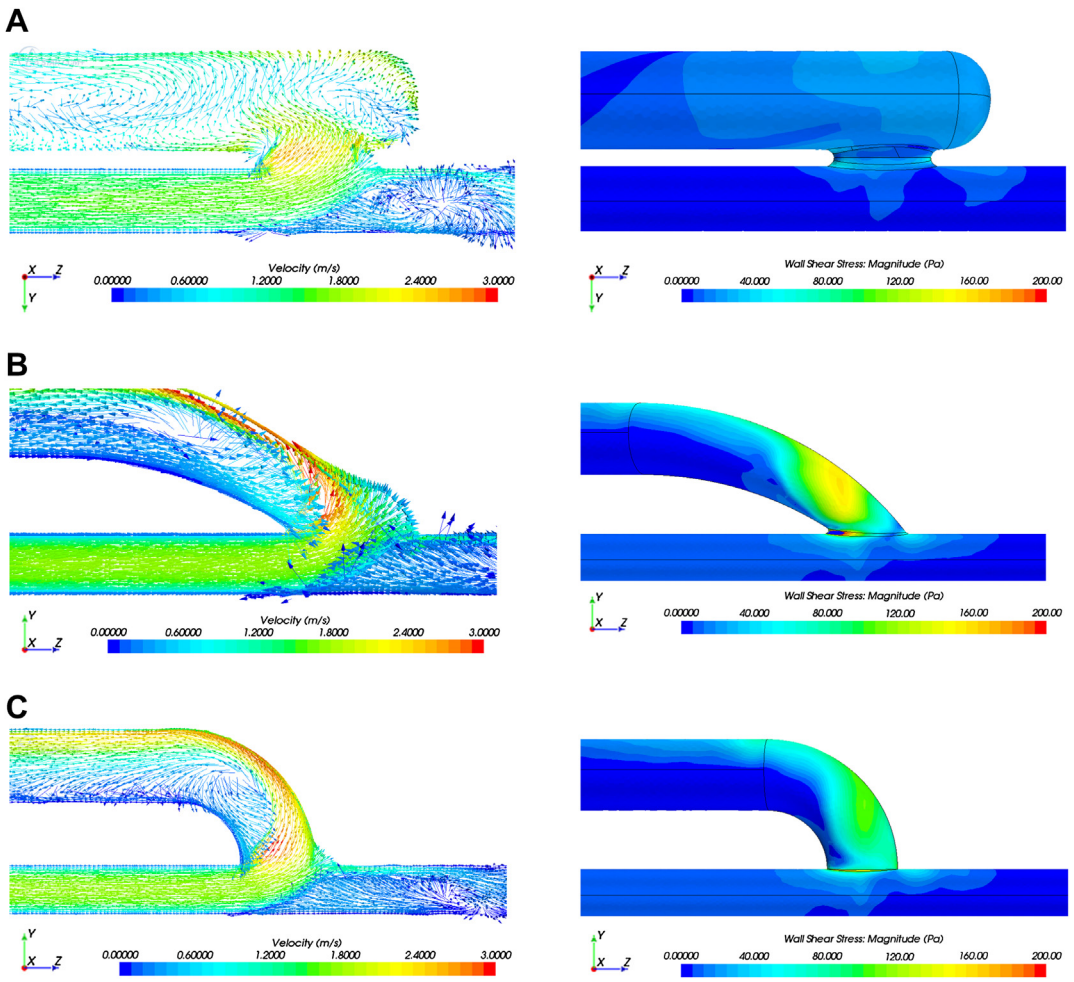

Fig 4. Paired velocity vector and wall shear stress (WSS) diagrams at a constant flow rate of 900 mL/min for 4 + 6 vein-pair models of side-to-side (STS) **(A)** and 45° **(B)** and 90° **(C)** end-to-side (ETS) anastomoses 6.0 × 4.0 mm in size. Note the uniform WSS in the STS configuration **(A)** compared with the marked variance in WSS in the 45° and 90° ETS configurations. The areas of low WSS (*blue*) adjacent to high WSS (*green/yellow/red*) in the proximal venous outflow of the 45° and 90° ETS configurations are prone to intimal hyperplasia.

Summing up the clinical application of CFD in the AVF anastomosis, a STS anastomosis with a length at least 1.5 times the arterial diameter would provide adequate flow and the most uniform WSS. With respect to steal phenomenon, ETS fistulas with an angle of 45° would prevent reverse arterial outflow, but with a potential increase in intimal hyperplasia. Usage of STS anastomosis is associated with unique anatomic requirements that are found frequently at the snuffbox and elbow.

Study limitations. The current study provides a theoretical view of the AVF anastomosis. Missing are many nuances of the surgical AVF such as vessel disease, amount of dissection, vessel tension, twisting and compliance, patient blood pressure, and cardiac output. The models used cannot account for all the potential variables in actual fistulas. The models are static and represent a snapshot in the life of a fistula. Soon after fistula creation in healthy vessels, a 3-mm artery and 3-mm vein are likely to become a 4-mm artery and 6-mm vein, and this was one reason for evaluating these two sizes of vessels; resulting increase in flow was not unexpected, although realistic changes in vessel size, shape, and compliance could not be modeled. The anastomoses evaluated were all elliptical, whereas in real life a variety of shapes are possible. A limited flow range of 600 to 1200 mL/min was used to represent flows potentially achievable in the vessel sizes modeled and suitable for dialysis. Very low or high flows may have a significant impact on AVF thrombosis, intimal hyperplasia, and aneurysm formation. Vessel compliance and surface characteristic are considered the same for arteries and veins, which represents the in vivo situation poorly. Putting into practice the data and concepts from this study will ultimately require verification in vivo with animal or human data. Although the STS anastomosis may have desirable characteristics in terms of

flow and prevention of intimal hyperplasia, its value remains to be demonstrated. The value of this study is that it suggests novel ways to achieve improved results.

CONCLUSIONS

Computational fluid dynamic analysis of the arteriovenous fistula has provided useful insights into pressure, flow, and WSS characteristics and the effect of anastomosis size, type, and angle as well as proximal venous outflow and arterial outflow. As for the general observations made, (1) pressure drop across the anastomosis is inversely proportional to CSA and proportional to arterial inflow; (2) anastomotic CSA is inversely proportional to pressure drop across the anastomosis and proportional to venous outflow; (3) the anastomotic configuration can significantly affect pressure drop and venous outflow; (4) the pressure drop is most prominently affected by anastomotic angle; and (5) venous outflow was fairly consistent across configurations with the exception of the open STS configuration, which had increased venous outflow. The STS and 90° ETS configurations have similar pressure and venous outflow characteristics, with the potential for reversed arterial outflow with larger anastomoses. The 45° ETS anastomosis produces less flow for a given CSA but resists reversed arterial outflow. The STS configuration has the most uniform WSS profile, which should lead to decreased intimal hyperplasia, and is followed by 45° end-to-side configuration; the least uniform WSS profile is provided by the 90° end-to-side configuration.

AUTHOR CONTRIBUTIONS

Conception and design: JH, BK
Analysis and interpretation: JH, BB, BK
Data collection: JH, BB, BK, DW
Writing the article: JH, BB
Critical revision of the article: JH, BB
Final approval of the article: JH
Statistical analysis: JH, BB
Obtained funding: JH
Overall responsibility: JH

REFERENCES

1. Krishnamoorthy MK, Banerjee RK, Wang Y, Zhang J, Roy AS, Khoury SF, et al. Hemodynamic wall shear stress profiles influence the magnitude and pattern of stenosis in a pig AV fistula. Kidney Int 2008;74:1410-9.
2. Van Canneyt K, Pourchez T, Eloot S, Guillame C, Bonnet A, Segers P, et al. Hemodynamic impact of anastomosis size and angle in side-to-end arteriovenous fistulae: a computer analysis. J Vasc Access 2010;11:52-8.
3. Bharat A, Jaenicke M, Shenoy S. A novel technique of vascular anastomosis to prevent juxta-anastomotic stenosis following arteriovenous fistula creation. J Vasc Surg 2012;55:274-80.
4. Niemann AK, Thrysoe S, Nygaard JV, Hasenkam JM, Petersen SE. Computational fluid dynamics simulation of a-v fistulas: from MRI and ultrasound scans to numeric evaluation of hemodynamics. J Vasc Access 2012;13:36-44.
5. Ene-Iordache B, Mosconi L, Remuzzi G, Remuzzi A. Computational fluid dynamics of a vascular access case for hemodialysis. J Biomech Eng 2001;123:284-92.
6. Krishnamoorthy M, Roy-Chaudhury P, Wang Y, Sinha Roy A, Zhang J, Khoury S, et al. Measurement of hemodynamic and anatomic parameters in a swine arteriovenous fistula model. J Vasc Access 2008;9:28-34.
7. Niemann AK, Udesen J, Thrysoe S, Nygaard JV, Frund ET, Petersen SE, et al. Can sites prone to flow induced vascular complications in a-v fistulas be assessed using computational fluid dynamics? J Biomech 2010;43:2002-9.
8. Ramacciotti E, Galego SJ, Gomes M, Goldenberg S, De Oliveira Gomes P, Pinto Ortiz J. Fistula size and hemodynamics: an experimental model in canine femoral arteriovenous fistulas. J Vasc Access 2007;8:33-43.

Submitted Jul 29, 2012; accepted Oct 3, 2012.

Additional material for this article may be found online at www.jvascsurg.org.

APPENDIX (online only)

The system of laminar Navier-Stokes equations was applied to the discretized model via the steady-state continuity

$$\nabla(\vec{u}) = 0 \tag{1}$$

and momentum equations

$$\rho\vec{u}\nabla(\vec{u}) = -\nabla p + \nabla\bar{\bar{\tau}} \tag{2}$$

where u (m/s) is the fluid velocity, $\rho = 1050$ kg/m^3 is the density, and τ (Pa) is the viscous stress tensor, given by

$$\tau^{ij} = 2\mu D^{ij} - \frac{2}{3}\mu\delta^{ij}\frac{\partial u^i}{\partial x^i} \tag{3}$$

where $\mu = 3.5$ mPa·s is the fluid dynamic viscosity assumed to be Newtonian, δ is the Kronecker delta, and x^i (m) is the Cartesian coordinate ($i = 1$ stays for x, $i = 2$ for y, and $i = 3$ for z).

$$D^{ij} = \frac{1}{2}\left(\frac{\partial u^i}{\partial x^j} + \frac{\partial u^j}{\partial x^i}\right) \tag{4}$$